Gazi Üniversitesi
Fen Bilimleri Dergisi
PART C: TASARIM VE TEKNOLOJİ

Gazi University
Journal of Science
PART C: DESIGN AND TECHNOLOGY

GU J Sci, Part C, 12(3): 639-661 (2024)

A Faster Active Package to Cell Balancing of Battery Management System using Isolated Cuk Converter with Switch Matrix

Alperen UĞURLUOĞLU[1*] Ahmet KARAARSLAN[1]

[1]*Ankara Yıldırım Beyazıt University, Faculty of Engineering and Natural Sciences, Department of Electrical and Electronics Engineering, Ankara, Turkey*

Article Info

Research article
Received: 21/05/2024
Revision: 15/08/2024
Accepted: 03/09/2024

Keywords

Cell Balancing
BMS
Isolated CUK Converter
Switch Matrix
Package to Cell

Makale Bilgisi

Araştırma makalesi
Başvuru: 21/05/2024
Düzeltme: 15/08/2024
Kabul: 03/09/2024

Anahtar Kelimeler

Hücre Dengeleme
BMS
Izole CUK Dönüştürücü
Anahtar Matriksi
Paketten Hücreye

Graphical/Tabular Abstract (Grafik Özet)

A faster and cost-effective active package to cell balancing battery management system by using an isolated CUK converter and switch matrix is introduced in this study for the li-ion batteries that have charge unbalance when they are uncontrolled. / Bu çalışmada, kontrolsüz olduklarında şarj dengesizliği yaşayan Li-ion bataryalar için izole CUK dönüştürücü ve anahtar matrisi kullanılarak daha hızlı ve maliyet etkin bir aktif paket hücre dengeleme batarya yönetim sistemi tanıtılmıştır.

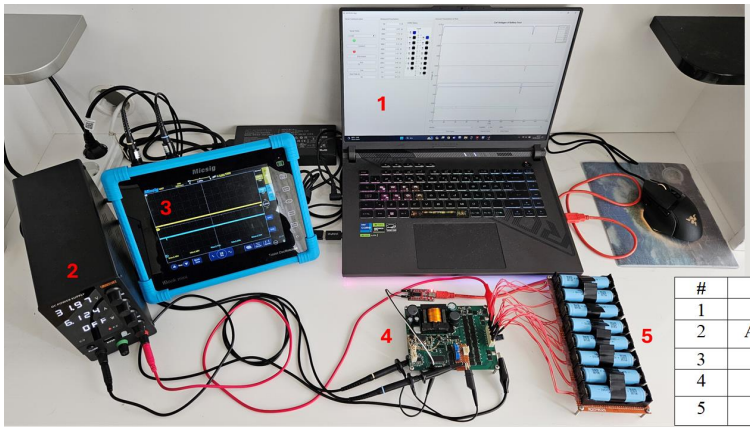

#	Name
1	BMS user interface
2	Adjustable power supply
3	Oscilloscope
4	Proposed Topology
5	Battery package

***Figure A**: The experimental setup of the proposed balance topology /**Şekil A:**.*
Önerilen dengeleme topolojisinin deneysel kurulumu

Highlights (Önemli noktalar)

- *This study highlights high balancing speed and a cost-effective active balancing method. / Bu çalışmada yüksek dengeleme hızı ve maliyet etkin bir aktif dengeleme yöntemi vurgulanmaktadır.*
- *High power capacity isolated CUK converter and multi-selection capable switch matrix are proposed. / Yüksek güç kapasiteli izole CUK dönüştürücü ve çoklu seçim yeteneği olan anahtar matriksi önerilmiştir.*
- *A feasible control method has been established with a cell selective algorithm, which constitutes the most optimal balancing process. / En optimal dengeleme sürecini oluşturan hücre seçimli algoritma ile uygulanabilir bir kontrol yöntemi oluşturulmuştur.*

***Aim (Amaç):** In this study, it is aimed to complete the balancing process in a short time and cost effectively and to use maximum Li-ion battery performance. / Bu çalışmada kısa sürede ve maliyet etkin bir şekilde dengeleme işlemini tamamlayıp maksimum Li-ion batarya performansı kullanımı hedeflenmektedir.*

***Originality (Özgünlük):** By using an isolated CUK converter capable of providing high power transfer, the cell selective algorithm offers a high-speed and cost-effective solution. / Yüksek güç aktarımı sağlayabilen bir izole CUK dönüştürücü kullanımı ile beraber hücre seçimli algoritma yüksek hızlı ve maliyet etkin bir çözüm sunmaktadır.*

***Results (Bulgular):** This study has achieved the fastest balancing among the package-to-cell methods, with a value of 9.64 mV/min, and the most cost-effective method based on cost analysis. / Bu çalışmada paket-hücre yöntemleri arasında en hızlı dengeleme 9,64 mV/dakika değeriyle elde edilmiş olup, maliyet analizlerine göre en uygun maliyetli yöntemdir.*

***Conclusion (Sonuç):** Load balancing of eight series cells was achieved using battery management system constructed with active package-to-cell balancing method including isolated CUK converter and switch matrix. / İzole CUK dönüştürücü ve anahtar matrisi içeren aktif paketten hücreye dengeleme yöntemi ile oluşturulan batarya yönetim sistemi kullanılarak sekiz seri hücrenin yük dengelemesi sağlanmıştır.*

*Corresponding author, e-mail: alperen.ugurluoglu@gmail.com
DOI: 10.29109/gujsc.1487808

GU J Sci, Part C, 12(3): 639-661 (2024)

Gazi Üniversitesi
Fen Bilimleri Dergisi
PART C: TASARIM VE TEKNOLOJİ

Gazi University
Journal of Science
PART C: DESIGN AND TECHNOLOGY

http://dergipark.gov.tr/gujsc

A Faster Active Package to Cell Balancing of Battery Management System using Isolated Cuk Converter with Switch Matrix

Alperen UĞURLUOĞLU[1*] Ahmet KARAARSLAN[1]

[1]*Ankara Yıldırım Beyazıt University, Faculty of Engineering and Natural Sciences, Department of Electrical and Electronics Engineering, Ankara, Turkey*

Article Info

Research article
Received: 21/05/2024
Revision: 15/08/2024
Accepted: 03/09/2024

Keywords

Cell Balancing
BMS
Isolated CUK Converter
Switch Matrix
Package to Cell

Abstract

This paper proposes a faster active package to cell (P2C) balancing battery management system (BMS) by using a proportion-integration (PI) controlled isolated CUK converter (ICC) with a cell-selective switch matrix (SWM). The high power capability of the ICC and a SWM that has the ability to select each cell individually or multiple cells in series increase balance speed. In addition, the low cost analysis and small size comparisons of the proposed study are presented. BMS is applied to battery packs to monitor the voltage, current, temperature, and state of charge (SoC) values of each cell and provide the battery pack with the ability to operate in a safe zone. One of the battery problems is that each battery cell in the pack does not contribute energy equally to the entire pack. Li-ion batteries that are used in this paper also suffer from this problem due to their higher energy density than other batteries. Therefore, a balancing operation is needed for the voltage and SoC of each cell. According to the average of battery cells, the entire pack charges the selected lower cells by converting the energy through ICC and switching the lower energized cells. Due to the isolation, the energy can be transferred from pack to cell. The proposed study is simulated in MATLAB Simulink and then implemented experimentally. The tests are conducted as an idle state balance operation, and the experimental tests show that the balancing operation requires 1170 seconds to balance a 10% SoC difference and 3033 seconds to balance a 55% SoC difference. The experimental studies produce a balancing speed of 9.64 mV/min with 81.98% efficiency. Finally, the result of the proposed study is compared with the other P2C methods in the literature. The comparison also showed that the proposed study is a cost effective solution.

İzole Cuk Dönüştürücü ve Anahtar Matrisi Kullanılarak Daha Hızlı Paketten Hücreye Dengeleyen Batarya Yönetim Sistemi

Makale Bilgisi

Araştırma makalesi
Başvuru: 21/05/2024
Düzeltme: 15/08/2024
Kabul: 03/09/2024

Anahtar Kelimeler

Hücre Dengeleme
BMS
Izole CUK Dönüştürücü
Anahtar Matriksi
Paketten Hücreye

Öz

Bu makale, hücre seçici anahtar matrisi (SWM) ile proportion-integration (PI) kontrollü izole CUK dönüştürücü (ICC) kullanarak daha hızlı bir aktif paket hücre (P2C) dengeleme batarya yönetim sistemi (BMS) önermektedir. ICC'nin yüksek güç kapasitesi ve her bir hücreyi ayrı ayrı veya seri halde birden fazla hücreyi seçme yeteneğine sahip bir SWM, dengeleme hızını artırır. Ek olarak, önerilen çalışmanın düşük maliyet analizi ve küçük boyut karşılaştırmaları sunulmaktadır. BMS, her bir hücrenin voltajını, akımını, sıcaklığını ve şarj durumu (SoC) değerlerini izlemek ve batarya paketine güvenli bir bölgede çalışma yeteneği sağlamak için batarya paketlerine uygulanır. Batarya sorunlarından biri de paketteki her hücrenin tüm pakete eşit şekilde enerji sağlamamasıdır. Bu makalede kullanılan Li-ion bataryalar de diğer bataryalara göre daha yüksek enerji yoğunlukları nedeniyle bu sorundan muzdariptir. Bu nedenle, her bir hücrenin voltajı ve SoC'si için bir dengeleme işlemi gereklidir. Batarya hücrelerinin ortalamasına göre batarya paketi enerjisi, ICC aracılığıyla dönüştürülerek seçilen daha düşük enerjili hücreleri şarj eder. İzolasyon sayesinde, enerji paketten hücreye aktarılabilir. Önerilen çalışma MATLAB Simulink'te simüle edilmiş ve ardından deneysel olarak uygulanmıştır. Testler boştaki durum dengeleme işlemi olarak yürütülmüştür ve deneysel testler, dengeleme işleminin %10 SoC farkını dengelemek için 1170 saniye ve %55 SoC farkını dengelemek için 3033 saniye gerektirdiğini göstermiştir. Deneysel çalışmalar, %81,98 verimlilikle 9,64 mV/dakika dengeleme hızı üretmiştir. Son olarak, önerilen çalışmanın sonucu literatürdeki diğer P2C yöntemleriyle karşılaştırılmıştır. Karşılaştırma ayrıca önerilen çalışmanın maliyet açısından etkili bir çözüm olduğunu göstermiştir.

*Corresponding author, e-mail: alperen.ugurluoglu@gmail.com
DOI: 10.29109/gujsc.1487808

1. INTRODUCTION (GİRİŞ)

In recent years, the electrification of electrical vehicles, marine vehicles and aerospace vehicles has become important because the electrical features of the vehicles increase each day. [1] According to the latest statistics, transport vehicles that use fossil fuels were responsible for 26% of the total greenhouse gas emissions of Saudi Arabia in 2019. [2] For those reasons, the need for energy storage systems is increasing to supply the required energy and reduce greenhouse gas emissions. One of the energy storage solutions is rechargeable batteries with lead-acid, nickel, or lithium electrochemistry. [3-5] Lithium batteries are the most commonly used rechargeable battery type recently for electrical vehicles, marine vehicles and aerospace vehicles due to their features of high power density, high current capacity, low maintenance and no memory effect. [6-8] However, rechargeable batteries must operate in a safe operating region because overcharging, over discharging, battery cell voltage unbalance and overheating conditions are harmful for batteries and may cause severe damage if they are not monitored. [9-11]

Battery charging and discharging periods may cause a battery voltage unbalance among the series connected battery cells over time. This leads to an overcharge or undercharge of a few battery cells in the battery pack. The overcharge of the battery causes overheating and even thermal runaway. On the other hand, overcharging a battery causes a reduction in its lifecycle and the even death of the battery cell. [12] Therefore, the BMS is used to balance the cell voltages and operate batteries with safe and higher performance.

Miscellaneous methods are presented and implemented to provide balancing operations among the battery cells. These are mainly active and passive balancing methods in the literature, as seen in Figure 1. [13-16] The passive balancing methods are fixed shunt and shunt switched resistor topologies. [17] The passive methods are very simple and have a very low cost since the resistor and switching elements are the only required components, but this method suffers from very low speed, inefficiency, and a heat problem due to the shunt resistors. On the other hand, active balancing methods offer high balancing speed due to active topologies, high efficiency due to charge transfer and fewer heat problems due to the nonexistence of shunt resistors. The cell to cell (C2C) [18-22] methods can transfer the excess charge either adjacent-cells to adjacent-cells or any-cell to any-cell. The C2C method provides moderately fast and highly efficient topologies such as switched capacitor, CUK converter and quasi resonant converter. However, the complexity of the C2C topologies is high because of the number of switching elements and passive components. Therefore, the cost and size of these topologies become high. The cell to pack (C2P) [15-16, 23-24] methods in the literature aim to transfer the charge from overcharged battery cells to the entire battery pack. The multi-winding forward transformers or unidirectional flyback converters are implemented in the literature as C2P balancing methods. The C2P methods are more cost effective and smaller in size than the other active methods. However, their balance speed is not as good as P2C methods, and their efficiency is moderate while their complexity is high due to the existence of a multi winding transformer and many switches.

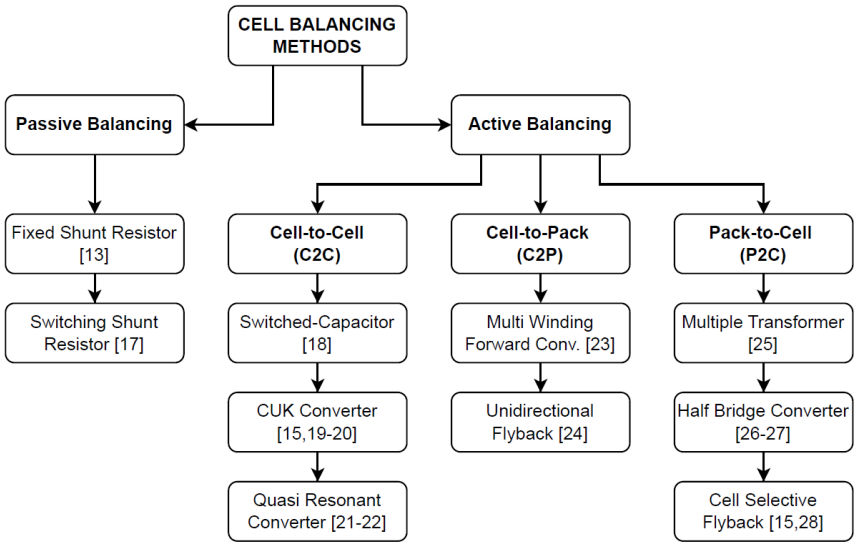

Figure 1. Chart of cell balancing methods (Hücre dengeleme yöntemleri çizelgesi)

The P2C method aims to transfer energy from the battery pack to the low-charged battery cells. The P2C method has the highest balance speed ability among the active methods. High-power balancing can be provided for large battery packages. In contrast, the efficiency and cost effectiveness are lower than the C2C and C2P studies. In terms of the P2C method, multiple transformers, cell-selective flyback or half-bridge topologies are presented in the literature. The multiple transformer topology requires separate transformers for each cell. [25] Also, the multi-winding transformer based half bridge converter topology takes up more space as the number of cells increases. [26] High balancing speed and high efficiency can be achieved by these topologies, but their high cost, high complexity and large size are their drawbacks. Another voltage multiplier based half bridge converter topology has the advantages of high balance speed, being relatively efficient and being lower in complexity due to the reduced switch count. [27] Conversely, the amount of passive components increases very much, and causes high cost and large size, as well. On the other hand, a cell-selective flyback converter transfers energy to the relevant cells with two transformers and a switch matrix that allows the selection of cells individually. [28] Even if the cell selected flyback converter provides less current and causes slow balance speed due to the low power design of the presented study, the cell selected flyback converter topology has an efficient, moderately simple, cost effective and medium sized topology among the P2C methods. Therefore, high power capable dc-dc converters are researched in the literature for faster performance. [29] The high current capability for faster balancing and high efficiency can be achieved by the push-pull, full bridge and half bridge converters. However, their complexity and cost are very high. Also, the size is large. Therefore, faster and more efficient topologies are researched by considering complexity, cost and size.

Battery balancing in literature requires the utilization of strategies such as battery cell terminal voltages, SoC, or capacity to implement a balance algorithm. [33] The strategy of monitoring battery cell terminal voltages is conventional, practical, and easy to implement. Nevertheless, this approach may suffer from an imbalance issue due to variations in the internal resistance and capacity of the battery cells caused by aging. Another approach is to consider the SoC levels of battery cells. This strategy is robust against the effects of aging and disturbances thanks to its dynamic balancing operation. Nevertheless, the computational effort is high. As a last strategy, the total capacity maximizes the energy utilization of a battery pack. Nevertheless, the implementation of this strategy in real-time requires a significant computing effort for the BMS.

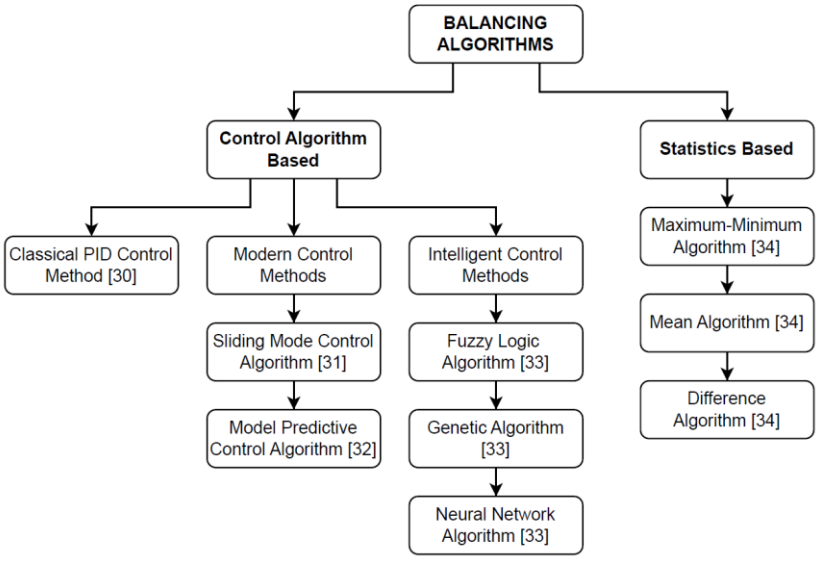

Figure 2. The balancing algorithms in the literature (Literatürdeki dengeleme algoritmaları)

Figure 2 provides a comprehensive list of the balancing algorithms provided in the literature. The adaptive PID controller, modern methods, and intelligent methods ensure robust control over both linear and nonlinear battery balancing operations. [30-33] Furthermore, the states of repeated balancing and overbalancing are eliminated. Nevertheless, these methods require complicated

mathematical models, significant computational effort, or data training. In contrast, the statistical algorithms of maximum-minimum, mean, and difference algorithms offer simpler implementation, lower computational effort, and higher accuracy. [34] Furthermore, these methods are widely applied. Nevertheless, the statistical algorithms may encounter repeated balancing and overbalancing issues. Besides, the proposed algorithm is also derived from the mean algorithm. The proposed algorithm constrains the balance operation by employing a threshold to prevent overbalancing. Additionally, a periodic operation function is implemented in the cell selective algorithm (CSA) algorithm to solve the problem of repetitive balancing, as shown in Figure 8.

In this study, a faster and more cost effective active P2C balancing BMS that can select the cells with the SWM, provide power transfer with the ICC is proposed. The proposed PI controlled ICC provides high current application, which results in high speed and low balance time. [35] Moreover, the SWM can be configured to select up to 4 cells for ICC, thus, high power balancing, expanded cell control and easier cell selection are provided. The proposed CSA monitors the voltage, current and SoC parameters of each cell and performs an optimal balancing operation in case of an imbalance. On the other hand, the proposed topology is cost effective among the P2C methods and offers a compact size of practical circuitry. The working principle, representative figures, calculations and explanation of the CSA algorithm are given in Section 2. The implementation and the results of the simulation are given in Section 3. The experimental study is presented in Section 4 by including the experimental implementation, SoC estimation, efficiency calculation, design performances, the results of balancing operations and the comparison with other P2C topologies. Finally, Section 5 includes the conclusion of the study.

2.METHODOLOGY OF BMS TOPOLOGY (BMS TOPOLOJİSİNİN METODU)

Recently, the battery packages that are used in real applications such as electrical land vehicles, marine vehicles, and aircraft have increased as the electrification trend increases. As a result, the balancing operation of the BMS topologies requires longer time to complete, which constrains maximizing battery capacity and health. [33] Therefore, higher balancing speed and the high current capability of the balancing topologies are required. On the other hand, the balancing topology needs to be cost effective and simpler. Consequently, the proposed ICC and SWM topologies are utilized for high balancing speed and low cost.

2.1. Working Principle of ICC (ICC çalışma prensibi)

The proposed balance topology is composed of ICC, SWM and a BMS controller that are given in Figure 3 (Proposed topology) and in Figure 6 (Whole system). One parallel and 8 series battery cells are used as a battery package. The Li-ion electrochemistry rechargeable battery cells (B [1:8]) are selected in this study [36].

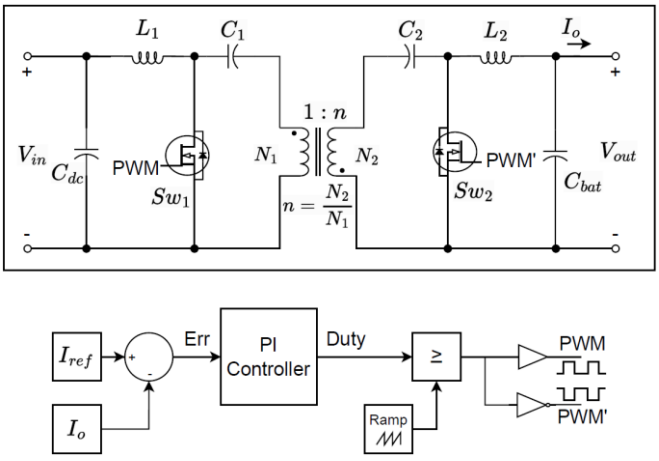

Figure 3. The proposed ICC topology and PI controller (Önerilen ICC topolojisi ve PI kontrolcü)

The ICC is composed of magnetic inductors (L_1, L_2), series capacitors (C_1, C_2), switching MOSFETs (Sw_1 and Sw_2), filter capacitors (C_{dc}, C_{bat}) and a transformer with a turns ratio of N_1/N_2 as seen in Figure 3.The ICC provides isolation to enable P2C power transfer and provides high power balancing. After the PI controller is activated to drive ICC, the ICC operates in two states as shown in Figure 4 and Figure 5.

State 1 Operation: By turning Sw_1 MOSFET on and Sw_2 MOSFET off as in Figure 4, L_1 is charged by battery pack while the output is supplied by C_1, C_2, C_{bat} capacitors and L_2 inductor. The transformer is discharged while transferring the energy on C_1 to secondary side.

State 2 Operation: By turning Sw_1 MOSFET off and Sw_2 MOSFET on as in Figure 5, L_1 charges the C_1 capacitor, the transformer on the primary side and C_2 on the secondary side. The output is supplied by C_{bat} capacitor and L_2 inductor.

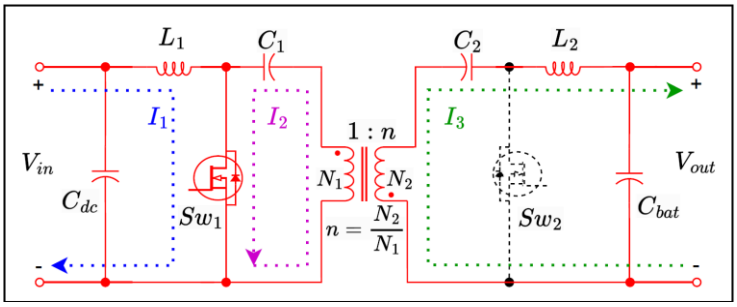

Figure 4. State 1 of proposed balance topology (Önerilen dengeleme topolojisinin 1. durumu)

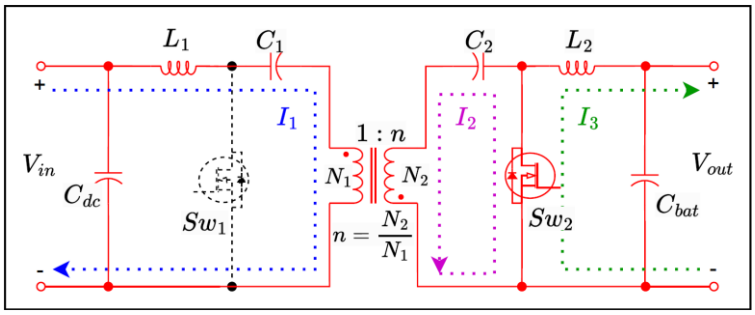

Figure 5. State 2 of proposed balance topology (Önerilen dengeleme topolojisinin 2. durumu)

2.2. Working Principle of SWM (SWM çalışma prensibi)

The ICC input is supplied by the battery package, and the output voltage can be adjusted to charge from 1 to 4 series battery cells according to what the battery balance algorithm needs. The ICC output terminals are connected to the SWM input. Also, the Li-ion battery cells are connected to SWM outputs individually. Thus, each battery cell can be selected. The SWM is composed of series diode (D_p[1:8], D_n[1:8]) and MOSFET (S_p[1:8], S_n[1:8]) branches. These branches provide to select positive and negative polarity of battery cells. The output of the ICC will be connected to the determined cell if the SWM is configured. The operation examples of SWM are given below. As seen in Figure 6 (a), the charge levels of B_8 and B_7 are lower than the average charge level. Therefore, the S_{p8} and S_{n7} MOSFET branches of SWM is turned on to select B_8 and B_7. On the other hand, the charge levels of B_4, B_3, B_2 and B_1 are lower than the average charge level. Therefore, the S_{p4} and S_{n1} MOSFET branches of SWM is turned on to select the cells from B_4 to B_1 as shown in Figure 6 (b).

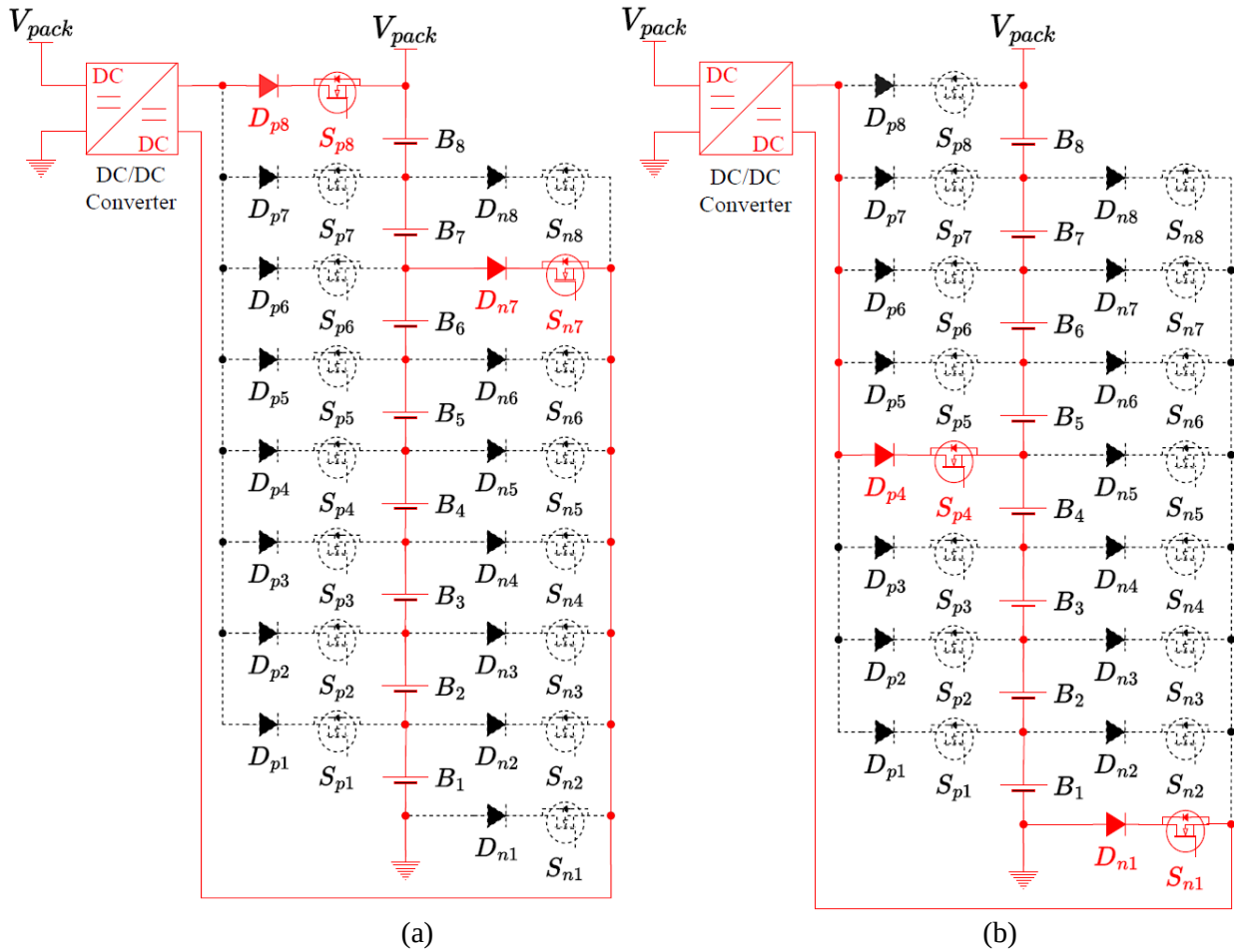

Figure 6. Selection configurations of SWM: (a) Two cells selection, (b) Four cells selection (SWM'in seçim yapılandırmaları: (a) iki hücre seçimi, (b) dört hücre seçimi)

2.3. BMS Controller (BMS kontrolcüsü)

As seen in Figure 7, the controller of the BMS monitors each battery cell voltage, input-output currents and temperature of the battery pack with the help of sensors in the proposed method. In idle state, the charge level of battery cells is monitored thanks to the SoC estimation algorithm, and lower-charged cells are determined in cases of an unbalanced condition. When a charge imbalance occurs among the battery cells, the controller enters into run state, configures SWM to select the determined cells with CSA, and enables the PI controller of the ICC for power conversion. Thus, the lower-charged cells are charged with the battery pack as P2C. In run state, the input and output of the ICC are measured to monitor how much current is flowed from the battery pack to the determined cells over time because the charge drop of the pack and the charge increase of the determined cells are required to finish the balancing operation.

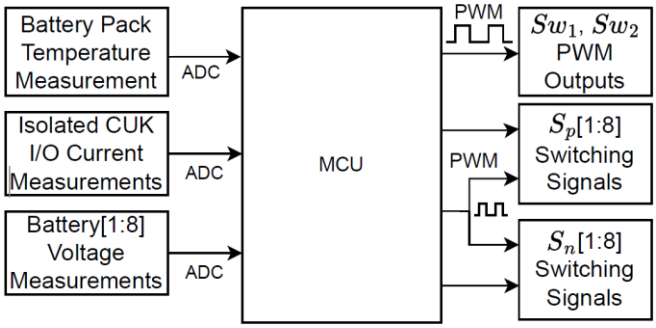

Figure 7. Controller block diagram (Kontrolcü blok diagramı)

2.4. Calculation of ICC Design Parameters (ICC tasarım parametrelerinin hesaplaması)

While operating the ICC in steady state condition, the input and output relationship of the converter is obtained as the equation (1).

$$V_{out} = \frac{n * V_{in} * D}{1 - D} \tag{1}$$

The output voltage, V_{out}, is equal to the transformer turns ratio, n, times input voltage, V_{in}, times duty cycle, D, divided by one minus D. The passive component values are calculated by considering the state 1 and state 2 of ICC that is shown in Figure 4 and Figure 5.

$$L_1 = \frac{V_{in} * D * T}{\Delta i_{l1}} = \frac{V_{in} * D * T}{\Delta i_{in}} \tag{2}$$

The value of L_1 inductor is equal to the input voltage, V_{in}, times duty cycle, D, times the switching period, T, divided by the change of current on L_1, Δi_{l1}, which is also equal to the change of input current, Δi_{in}, as obtained from the equation (2).

$$L_2 = \frac{V_{out} * (1 - D) * T}{\Delta i_{l2}} = \frac{V_{out} * (1 - D) * T}{\Delta i_o} \tag{3}$$

For the L_2 inductor, the equation (3) is obtained. The L_2 inductor equals to the output voltage, V_{out}, times duty cycle, D, times the switching period, T, divided by the change of current on L_2, Δi_{l2}, which is also equal to the change of output current, Δi_o.

$$L_m = \frac{V_{in} * D * T}{\Delta i_{Lm}} = \frac{V_{in} * D * T}{\Delta(i_{in} + n * I_o)} \tag{4}$$

The simplified equation (4) to calculate magnetizing inductance value of transformer, Lm, is equal to the input voltage, V_{in}, times duty cycle, D, times the switching period, T, divided by the change of current on L_m, Δi_{lm}, which is equal to $\Delta(I_{in} + n * I_o)$.

$$C_1 = \frac{I_{in} * (1 - D) * T}{\Delta V_{in}} \tag{5}$$

The C_1 capacitor value is obtained with the equation (5). The C_1 capacitor equals to the input current, I_{in}, times one minus duty cycle, D, times the switching period, T, divided by the change of voltage on C_1, ΔV_{c1}, which is also equal to the change of input voltage, ΔV_{in}.

$$C_2 = \frac{I_o * D * T}{\Delta V_o} \tag{6}$$

The C_2 capacitor value is obtained with the equation (6). The C_2 capacitor equals to the output current, I_o, times duty cycle, D, times the switching period, T, divided by the change of voltage on C_2, ΔV_{c2}, which is also equal to the change of input voltage, ΔV_{out}.

$$C_{bat} = \frac{\Delta i_{L2} * T}{8 * \Delta V_o} \tag{7}$$

The capacitance of the output capacitor, C_{bat}, is obtained with the equation (7). The C_{bat} capacitor equals to the change of current on L_2, Δi_{l2}, which is also equal to the change of output current, Δi_o, times duty cycle, D, times the switching period, T, divided by the change of voltage on C_{bat}, ΔV_{cbat}, which is also equal to the change of input voltage, ΔV_{out}, multiplied by 8.

The component values are calculated and implemented in the proposed topology as listed in Table 1. The MOSFETs and diodes are selected by considering their operation region in the balance circuit. The ICC MOSFETs are driven with 50 kHz PWM signals. The PWM outputs of the balance topology and UART output for the BMS user interface are provided, and the temperature, current and voltage measurements are monitored by a microcontroller. Nickel-enriched lithium nickel manganese cobalt oxide (LiNiMnCoO2) electrochemistry battery cells are used in this study. [37] The battery cells are 18650 packages. Their charge capacity is 2800 mAh, and voltage range is 4.25 V max and 2.5 V min.

Table 1. Design parameters (Tasarım parametreleri)

Parameter		Value
Input voltage (V_{in})		20 V to 33.6 V
Output voltage (V_{out})		0 V to 16.8 V
Max output power (P_o)		50.4 W
Switching frequency		50 kHz
Efficiency (η)		81.98 %
ICC MOSFETs (Sw_1, Sw_2)		BSC070N10NS5ATMA1 100V 80 A
SWM MOSFETs ($S_{p1:8}$, $S_{n1:8}$)		CSD18511Q5AT 40 V 100A
Diodes ($D_{p1:8}$, $D_{n1:8}$)		SVM1045VB 45V 10 A
Micro-controller		DSPIC33FJ16GS502
Battery	Package	8S
	Part number	ASPİLSAN INR18650A28
	Voltage	2.5V Min, 3.65V Nominal, 4.25 Max
	Capacity	2800 mAh
	Max. charge current	4A
	Max. discharge currents	14A
Primary inductance, L_1, ESR_{L1}		330uH, 326mΩ
Primary capacitance, C_1, ESR_{C1}		100 uF, 210mΩ
Secondary inductance, L_2, ESR_{L2}		330uH, 326mΩ
Secondary capacitance, C_2, ESR_{C2}		680uF, 45mΩ
Output capacitance, C_{bat}, ESR_{Cbat}		100 uF, 6mΩ
Transformer	L_m	116uH
	L_{lk}, R_{ser}	1.22uH, 90m Ω
	N_p/N_s	30:30
	Core	EPCOS B66359A ETD 29/16/10

ESR: *Equivalent series resistance*

2.5. The Design Explanation of CSA (CSA'nın tasarım açıklaması)

The CSA starts by sampling the open circuit voltages (OCV) of the battery cells as seen in Figure 8. Then, it calculates the average of these cell voltages for comparison with each other. Each battery cell voltage is compared with the average voltage of the cells. If all the battery voltages are close to the average voltage within a determined tolerance, the cell voltages are balanced, and the balance operation is passive. However, in the reverse situation, an unbalance is detected, and the balancing operation is activated.

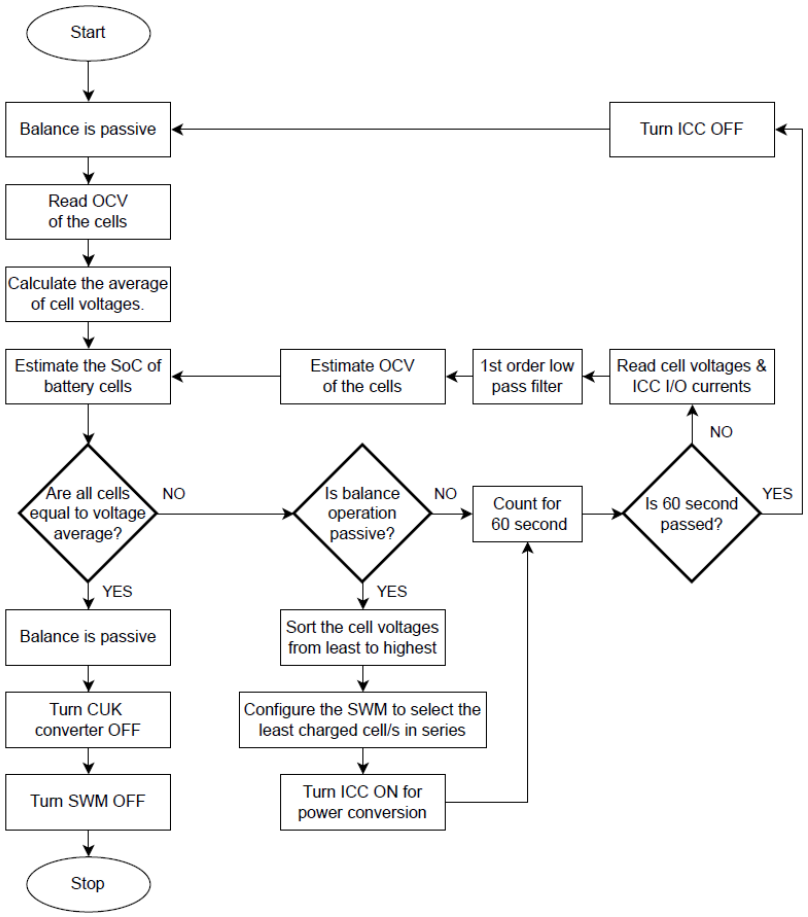

Figure 8. CSA battery balance algorithm (CSA batarya dengeleme algoritması)

The sampled cell voltages are sorted from the least to the highest. Thus, the least charged cell is determined. Moreover, the cells that are connected serially with the least charged cell are checked to see if they are below the average voltage of the cells. The least charged cell and its series cells that are below the average voltage are selected for balancing. Then, the SWM is configured for selected cells, and the ICC is turned on to start the power transfer as P2C. After the balance operation is started, the cell voltages, input and output currents of the ICC are monitored continuously. After low-pass filtration, the calculated voltage drops over battery cells are estimated and subtracted from each cell voltage to estimate the OCV. The obtained cell voltages are then used to calculate the SoC levels of the cells and compare them with the average cell voltage. If the cell voltages are balanced, balance operation is stopped by CSA. Otherwise, the balance operation continues. The time step of battery balance operation is determined as the optimum value of 60 seconds to be able to reconfigure the SWM safely and lessen the computational effort. The balance operation is periodically stopped to monitor the OCV of each cell, update the average voltage and sort the battery cell voltages for the next SWM configuration at the end of every 60 seconds. Then, the balance operation continues by activating ICC and configuring SWM.

3.SIMULATION RESULTS (SİMÜLASYON SONUÇLARI)

The proposed BMS balance topology is simulated in MATLAB Simulink before being verified experimentally. The balance operation proceeds in an idle state scenario. The voltage, current, and SoC inputs are observed in the simulation. The ICC output graphs, and the balance operation graphs are obtained.

3.1. Block Diagrams of BMS Topology (BMS topolojisinin blok diagramları)

The block diagrams of the proposed BMS balance topology in MATLAB Simulink are given in Figure 9, Figure 10 and Figure 11.

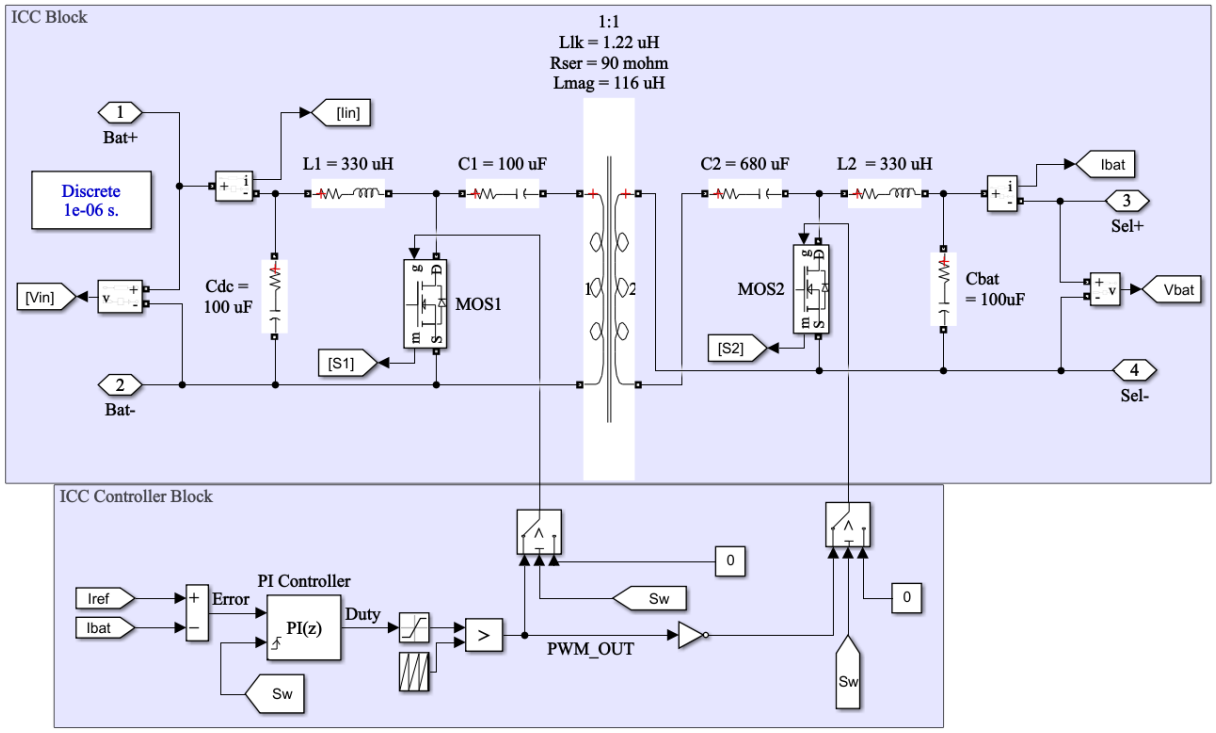

Figure 9. Block diagram of ICC and PI controller (ICC ve PI kontrolcünün blok diagramı)

The block diagrams of the ICC and PI controller are shown in Figure 9. The parameters of the simulation and the passive components of ICC are found in Table 1. The ICC is connected to the battery package terminals at the input, and the SWM selection terminals at the output. The terminals are also given in Figure 10. The switching elements of MOS_1 and MOS_2 are connected to the output of the PI controller. In addition, the PI controller can be started or stopped by S_w signal in simulation according to the need for balancing. After the PI controller receives an enable signal, the ICC starts to operate.

In the implemented simulation setup, idle state battery balancing operation is simulated with eight series connected battery cells. To test the functionality and the performance of the proposed BMS topology, two different conditions that are SoC difference and SoC sequence are combined. The SoC difference of the battery cells are configured as 10% and 43% in two different attempts to see the minimum and maximum operation scenarios. Also, the SoC level of the battery cells are adjusted in a random sequence in these two attempts to produce more challenging balance operation for the CSA.

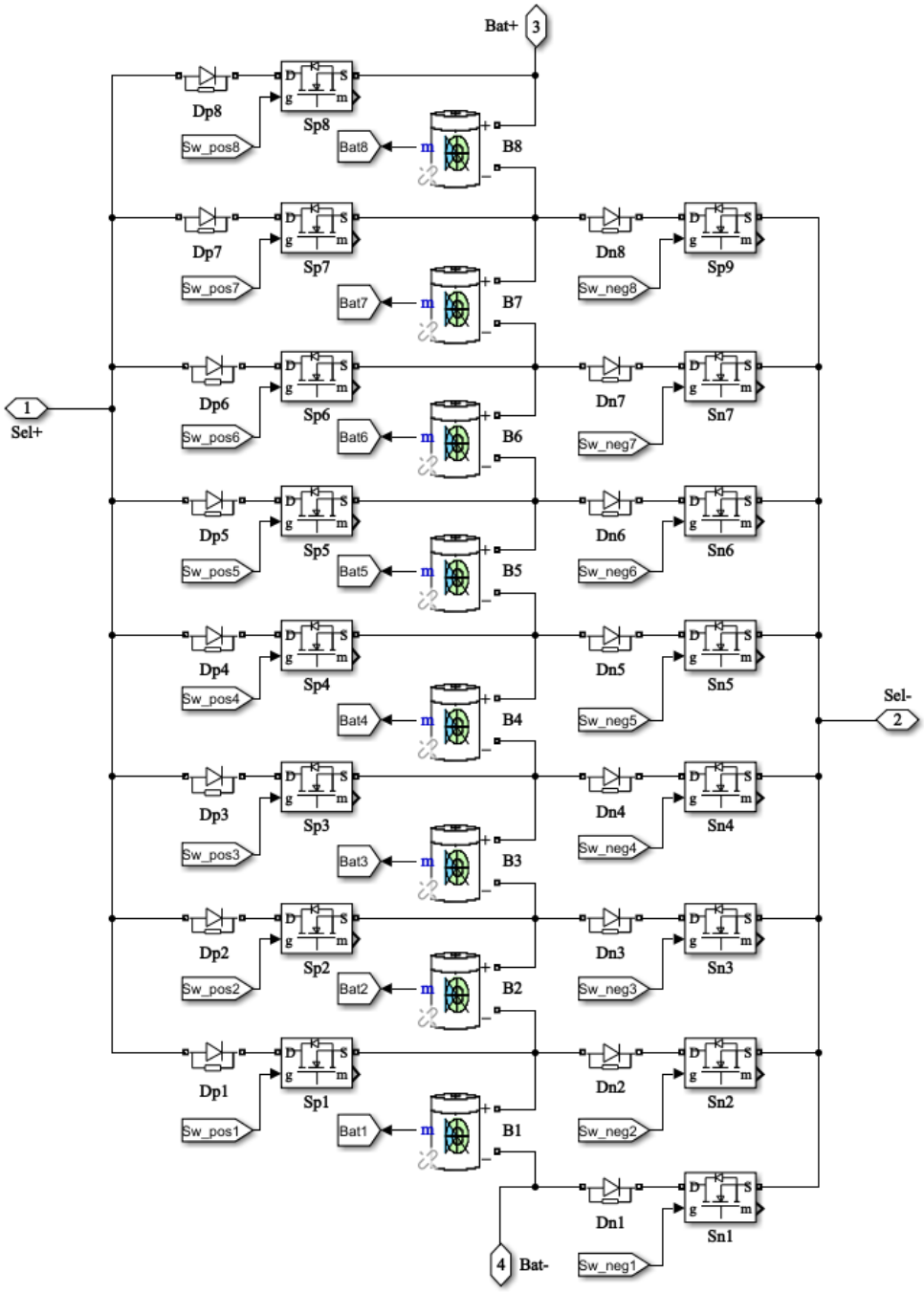

Figure 10. Block diagram of the SWM and batteries (SWM ve bataryaların blok diagramları)

The block diagrams of the SWM, BMS controller, and batteries are shown in Figure 10 and Figure 11. The batteries in Figure 10 are adjusted to 2.8 Ah and 3.65 V nominal voltage levels. Also, the SoC level of each battery cell is monitored in the battery pack. Each SWM switch is controlled by the BMS controller with 16-bit discrete signals. According to the selected battery cells, only one pair of the positive and negative switches is enabled, and the other switches are disabled. Furthermore, the BMS controller includes the CSA algorithm, thus, the gate signals of the SWM and PI controller of the ICC are controlled when there is a SoC imbalance. Also, the BMS controller has a time reference for the periodic operation of CSA.

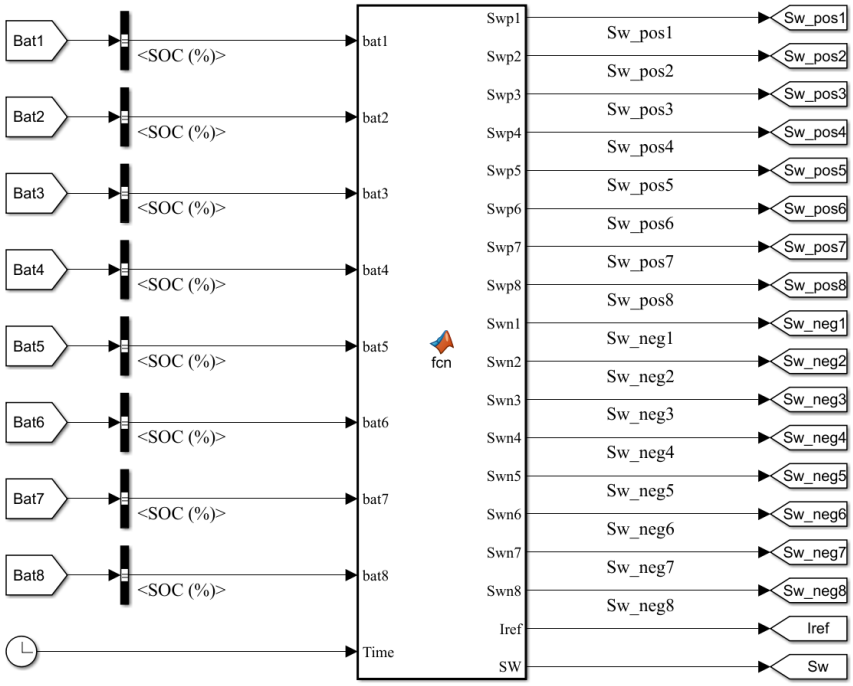

Figure 11. Block diagram of the BMS controller (BMS kontrolcüsünün blok diagramı)

3.2. ICC Outputs of Simulation (ICC simülasyon çıktıları)

The simulation of ICC produces the voltage and current outputs that are shown in Figure 12. While one battery cell is balancing, the output voltage is settled at the one cell charging voltage while the balance current is settled around 3A, as shown in Figure 12(a). Also, the current again settles around 3A, and the output voltage is settled at the four-cell charging voltage while four series cells are balancing, as shown in Figure 12(b).

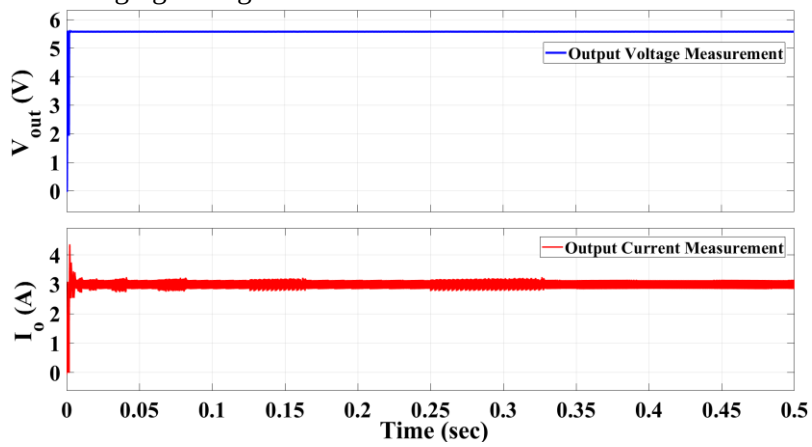

(a)

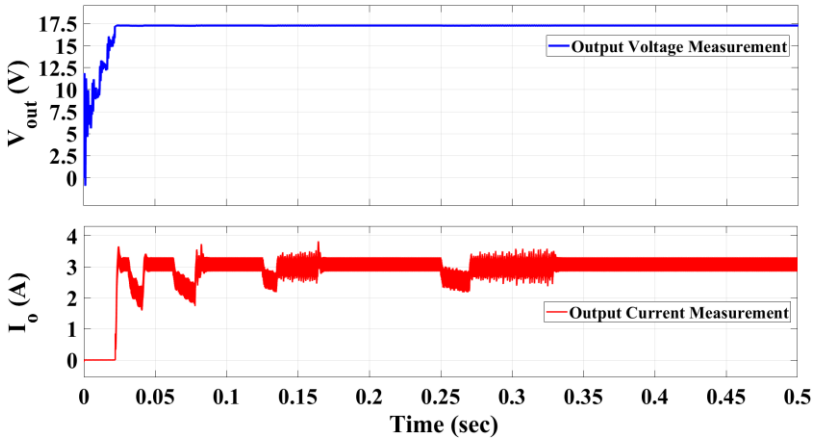

(b)

Figure 12. Cell balance outputs of simulation: (a) 1S cell balance, (b) 4S cell balance (Simülasyona ait hücre dengeleme çıktıları: (a) Bir seri hücre dengeleme, (b) 4 seri hücre dengeleme)

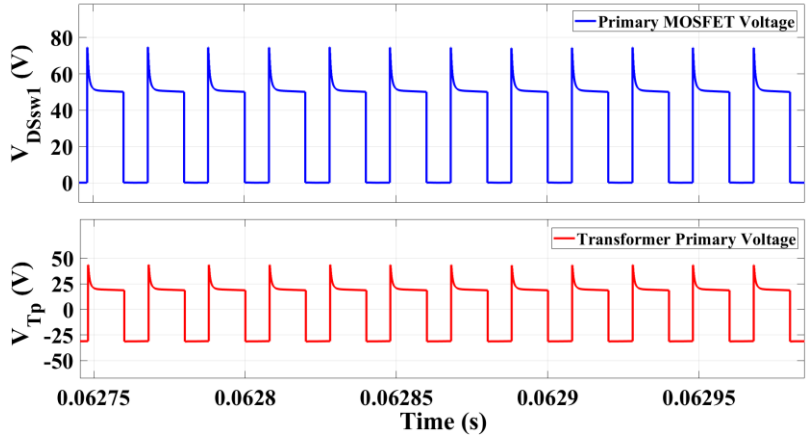

Figure 13. ICC voltage measurements in simulation (Simülasyondaki ICC voltaj ölçümleri)

While the ICC is operating at maximum power, the primary MOSFET voltage stress is equal to the sum of the input and output voltages. Also, it can reach up to 50 V, and a voltage spike can reach up to 75 V, as shown in Figure 13. On the other hand, the primary voltage of the transformer is equal to the input voltage for the on state and equal to the output voltage for the off state.

3.3. Simulation Outputs of Balancing Operation
(Dengeleme operasyonu simülasyon çıktıları)

The balance operation is simulated in MATLAB Simulink, and the final output is obtained as shown in Figure 14 The first simulation result of battery balance is shown in Figure 14 (a). The SoC levels of the battery cells are initially set to 59.5%, 61.5%, 56%, 59%, 57%, 66%, 62.5% and 65% from 8S to 1S. The SoC unbalance of the current configuration is 10% at maximum. In that situation, the balance operation is finished in a quarter of an hour, which is 15 minutes. The resulted SoC levels are 57±1%. The second attempt is shown in Figure 14 (b). The SoC levels of the battery cells are initially set to 70%, 35%, 30%, 27%, 55%, 50%, 38% and 65%, respectively. At the beginning, the SoC difference between the highest and lowest SoC is 55%. In the final situation, the SoC levels are in the range of 30% and 32%. The balance operation took an hour and 6 minutes.

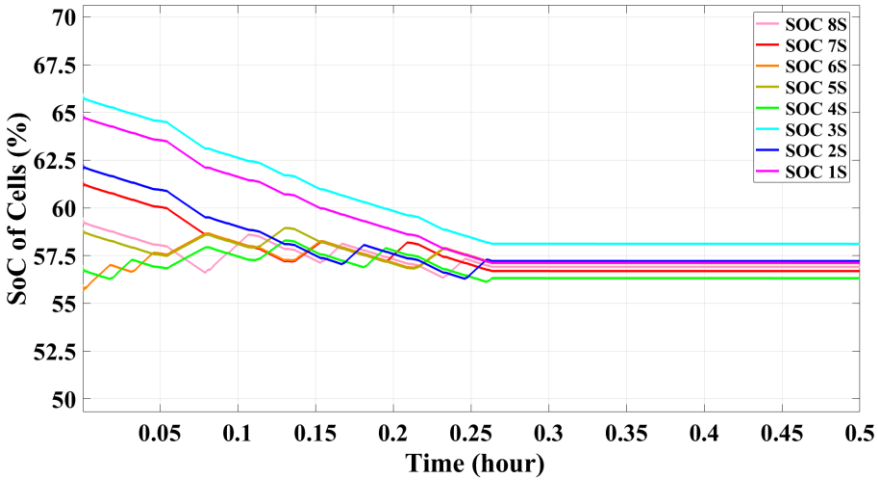

(a)

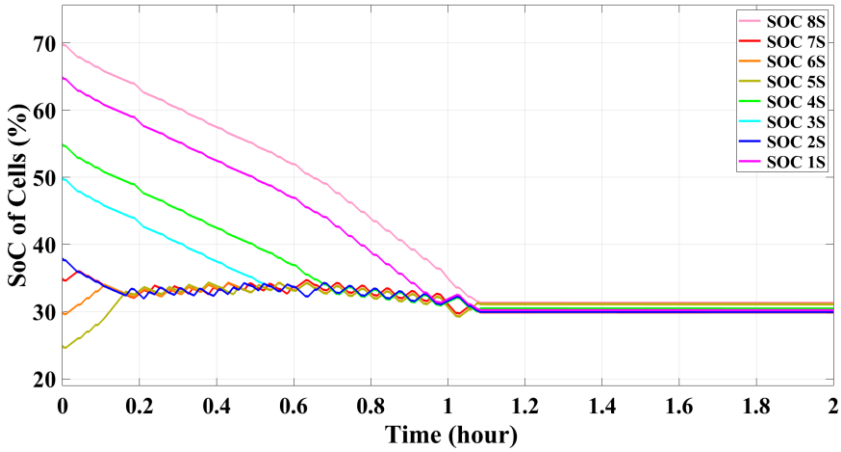

(b)

Figure 14. (a) First simulation result of battery balancing, (b) Second simulation result of battery balancing ((a) Batarya dengelemenin ilk simülasyon sonucu, (b) Batarya dengelemenin ikinci simülasyon sonucu)

4.EXPERIMENTAL RESULTS (DENEYSEL SONUÇLAR)

The proposed BMS balance topology is implemented as an experimental study to validate the simulation results. The voltage and SoC based balancing strategies are applied to an idle state battery balancing scenario. As a result, the operational ICC output graphs and balancing operation graphs are obtained.

4.1. Implementation of Test Setup (Test kurulumunun uygulanması)

The experimental study of the proposed topology is shown in Figure 15. The BMS topology is supplied by a power supply and the battery package. The input and output measurements are obtained by using an oscilloscope and a BMS user interface.

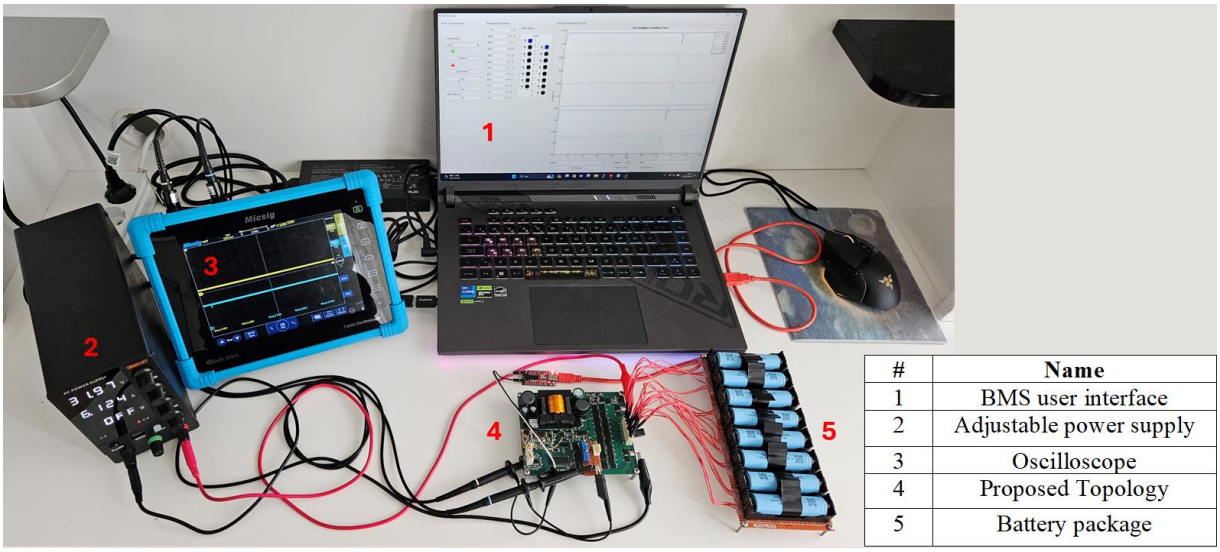

#	Name
1	BMS user interface
2	Adjustable power supply
3	Oscilloscope
4	Proposed Topology
5	Battery package

Figure 15 The experimental setup of the proposed balance topology (Önerilen dengeleme topolojisinin deneysel kurulumu)

4.2. Comparison and Calculation of SoC (SoC hesaplaması ve karşılaştırması)

The balancing operation of the BMS is completed at the point where the battery cell voltages and their charges are equal. Therefore, steady battery cell voltages and their charge levels need to be calculated. However, the battery cell voltages increase or decrease while charging or discharging due to the internal resistance of the battery cells. Consequently, the studies of SoC estimation methods are researched and gathered in Table 2. [8, 38, 39] Furthermore, their advantages and disadvantages are compared.

Table 2. Comparison of the SoC estimation methods in literature (Literatürdeki SoC tahmin yöntemlerinin karşılaştırması)

SoC Estimation Methods	Advantages	Disadvantages
OCV	Implementation is easy, high precision	Requires long rest times for steady OCV, Thus, only applicable for the idle state
Model-based SoC estimation	Online and precise SoC estimation while the battery is charging or discharging	Highly model dependent
Internal resistance	Offers simple Implementation	High precision of SoC estimation is provided only at the end of discharging
CC	Easy implementation is offered with low power consumption	Inaccurate estimation due to the uncertain disturbances, difficulties of initial SoC estimation that causes cumulative effect
KF	Estimates SoC accurately in existence of external disturbances	Requires complex mathematical models, has possibility to diverge due to the inaccurate models
NN	Capability of working in noisy or nonlinear conditions, High accuracy	Trained data requires high memory storage, high computational effort
Controller based observer	Offers high accuracy, stability and robustness for non linear conditions	Difficulty of obtaining controller parameters, high computational effort
The proposed hybrid model	Simple implementation and high precision, online SoC estimation while charging or discharging	Aging effect and uncertain disturbance dependent while online SoC estimation,

The first method of OCV uses the OCV versus SoC graph that is obtained by monitoring the voltage of the long rested battery cells. The model-based SoC estimation method requires a battery model, such as an electrochemical model or an equivalent circuit model to create an OCV-SoC look up table. The created look up table provides online SoC estimation while charging or discharging but this method is highly model dependent. The internal resistance method simply uses the DC voltage and current measurements to obtain the internal resistance of batteries to estimate the SoC. However, the measured resistance is in the mΩ range, so the calculations are accurate if the battery is discharging. The next method is coulomb counting (CC). This method is simply based on the integration of charging and discharging battery currents with respect to time. However, the initial SoC estimation is difficult and uncertain disturbances cause inaccuracies. The Kalman filter (KF) based methods offer dynamic estimation of SoC against uncertain disturbances and noises. A set of state equations is used in this method to out deviations and noises. However, the state equations are very complex to obtain. Another method is neural network (NN). This method takes the battery voltage and temperature as input and provides the SoC estimation output by applying the trained data. The controller based observer methods include controllers such as PI, sliding mode or fuzzy logic to observe the OCV precisely to obtain the SoC-OCV relationship.

The proposed hybrid method includes OCV and internal resistance. The simplicity and precision of the OCV method are combined with the internal resistance method. Thus, the change in cell voltage due to the internal resistance while charging or discharging is suppressed by the estimated internal resistance. Then, the look up table for the OCV-SoC graph is obtained and used in the balancing operation. However, the noise and temperature dependence are the same as in the OCV method. The calculations are started by discharging the battery cells from the maximum voltage level to the minimum voltage level with 3A and 0.6A current levels. The discharge curve of the battery cells is obtained as seen in Figure 16. These curves are used to obtain a look-up table for the estimation of the SoC level and internal resistance of battery cells, as seen in Figure 16 (a) and Figure 16 (b).

$$OCV_{cell} = V_{measured} + I_{cell} * R_{internal} \quad (8)$$

$$SoC_{cell}(\%) = \left(1 - \frac{DOD_{cell}\,(Ah)}{Capacity\,(Ah)}\right) * 100\% \quad (9)$$

While balancing the battery cells, the internal resistance curve is used to estimate the OCV of the cells that are charging or discharging. Thus, the OCV is estimated by using the measured cell voltages in equation (8). Also, depth of discharge (DoD) curve points of 3A are used to estimate the DoD level of OCVs by using the same equation. Thus, an estimated DoD curve is obtained against the OCV voltage and plotted in Figure 16(a). Then, the OCV of each cell is obtained by applying the curves in Figure 16(b). The obtained DoD is later used to estimate the SoC percent of each cell by applying the equation (9).

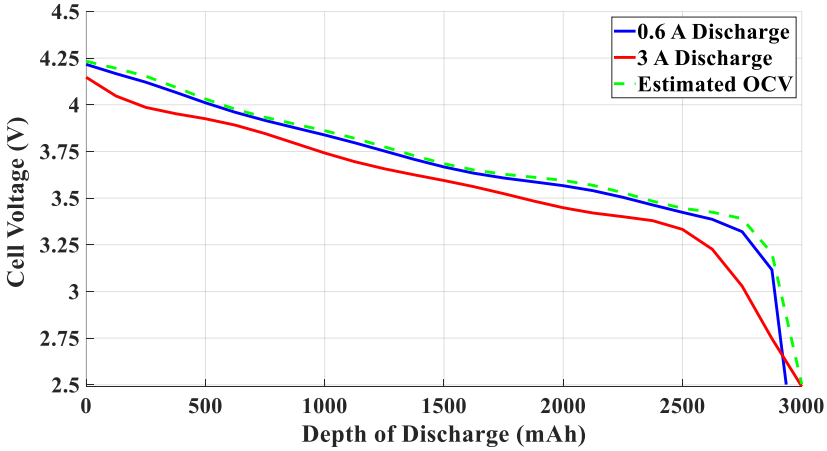

(a)

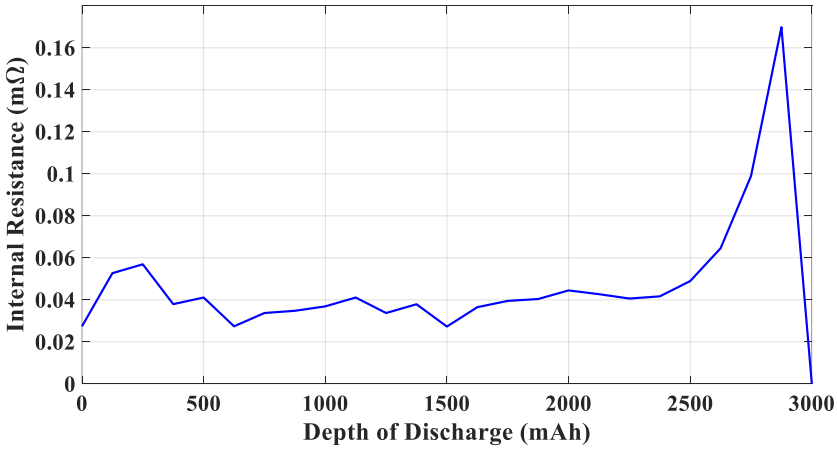

(b)

Figure 16. (a)The depth of discharge curves of the battery cells, (b) The internal resistance curve of the battery cells ((a) Batarya hücrelerinin deşarj durumu eğrileri, (b) Batarya hücrelerinin iç direnç eğrisi)

4.3. ICC Outputs of Experimental Study
(Deneysel çalışmanın ICC çıktıları)

The experimental study of ICC produces the voltage and current outputs that are shown in Figure 17. While one battery cell is balancing, the output voltage is settled at the one cell charging voltage while the balance current is settled around 3A, as shown in Figure 17 (a). Also, the current again settles around the 3A, and the output voltage is settled at the four-cell charging voltage while four series cells are balancing, as shown in Figure 17 (b).

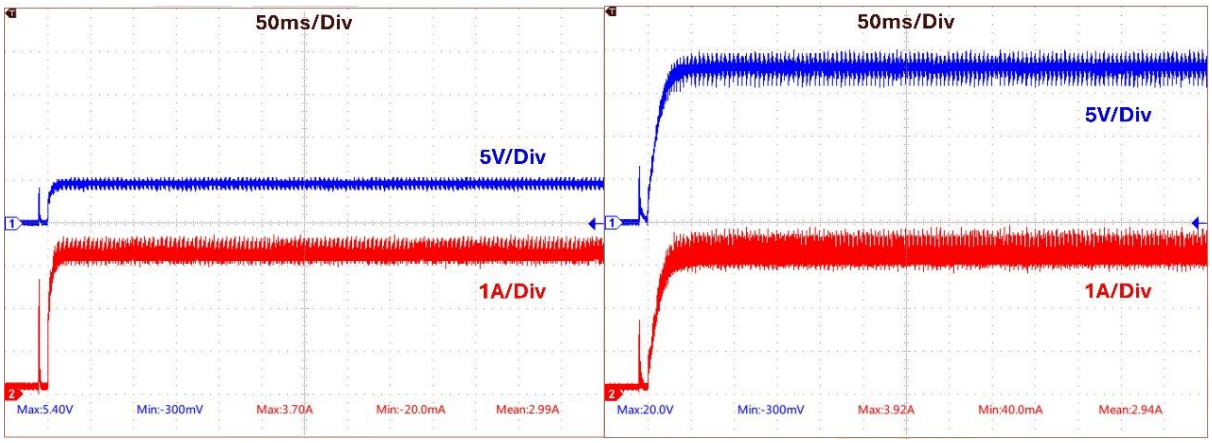

(a) (b)

Figure 17. Cell balancing outputs of experimental study: (a) 1S cell balance, (b) 4S cell balance (Deneysel çalışmanın hücre dengeleme çıktıları: (a) Bir seri hücre dengeleme, (b) dört seri hücre dengeleme)

At the maximum power of ICC operation, the primary MOSFET voltage stress is equal to the sum of the input and output voltages. Also, it can reach up to 50 V, and a voltage spike can reach up to 72 V, as shown in Figure 18. On the other hand, the primary voltage of the transformer is equal to the input voltage for the on state and equal to the output voltage for the off state. Also, it has a voltage spike level of 40.8 V.

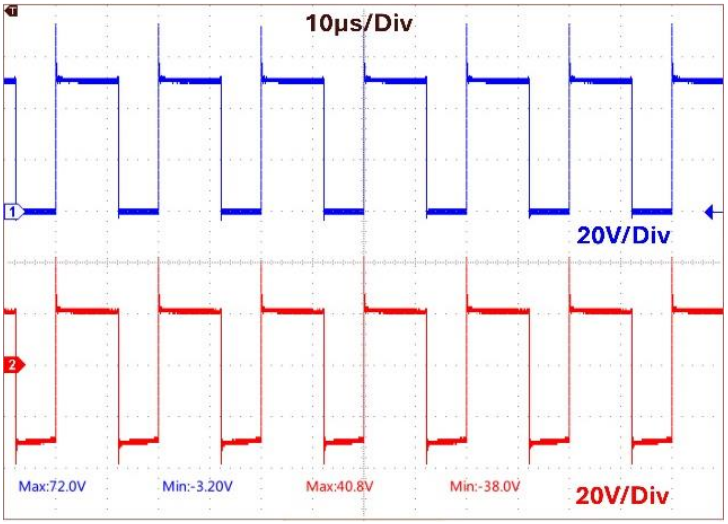

(b)

Figure 18. ICC voltage measurements of experimental study (Deneysel çalışmanın ICC voltaj ölçümleri)

4.4. Efficiency Calculation (Deneysel hesaplama)

The efficiency calculations in the literature are researched, and it is seen that there are four main methods of efficiency calculation. These are loss analysis [40], resistive loads [27], constant battery operation [26], and continuous balancing operation [21]. Since the working principle of the proposed CSA has momentary discontinuities, the continuous balancing operation is not satisfied. On the other hand, the loss analysis only gives theoretical results. Therefore, the resistive and constant battery operations are proper methods for this study. Among these methods, the constant battery operation is considered the optimal solution and selected to calculate the efficiency of the proposed topology.

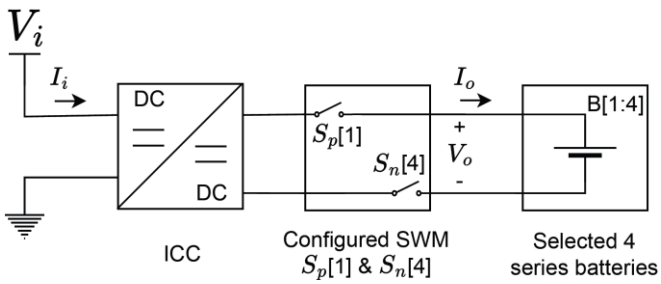

Figure 19. Block diagram of input and output measurements (Giriş ve çıkış ölçümlerinin blok diagramı)

The measurement locations of the current and voltages for both input and output are shown in Figure 19. The input voltage and selected cell voltages are kept constant, and an output current range is applied. These measurements are later used in equation (10) to calculate the efficiency points that correspond to each output current value. By collecting these efficiency points, an efficiency versus output current graph is obtained.

$$\eta\,(\%) = \frac{P_o * 100\%}{P_i} = \frac{V_o * I_o * 100\%}{V_i * I_i} \qquad (10)$$

The efficiency of the experimental study is measured on practical circuitry, as shown in Figure 20. The efficiency graph is measured by configuring the SWM output to have four series cells selected. Each cell voltage is adjusted around 3.8V and the ICC charges the selected cells with a range of current values from 1 A to 3.5A. Thanks to the MATLAB user interface, the current and voltage measurements of the input and output sides are sampled. Later, these parameters are used to calculate efficiency and a curve fitted graph is presented. As a result, the maximum efficiency of the experimental circuit is measured at 81.98% while the balance current is close to 3 A.

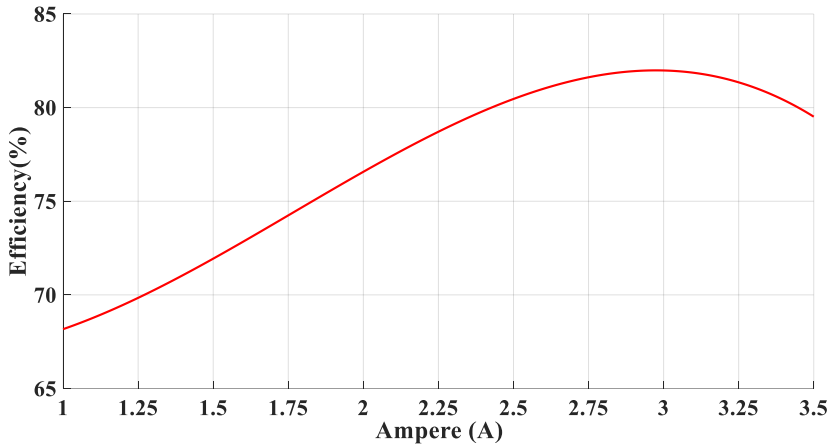

Figure 20. Efficiency of the proposed balance topology (Önerilen dengeleme topolojisinin verimi)

4.5. Experimental Outputs of Balancing Operation (Dengeleme operasyonunun deneysel çıktıları)

The balance operation data are collected in the BMS user interface that is designed in MATLAB. The collected data are later used to plot the experimentally implemented BMS topology results as shown in Figure 21. The first attempt at the experimentally implemented BMS topology is shown in Figure 21 (a). At the beginning, the battery cell voltages are 3.722 V, 3.728 V, 3.699 V, 3.720 V, 3.704 V, 3,794 V, 3,742 V and 3.791 V from 8S to 1S. The estimated SoC unbalance is 11.33% among the highest and lowest charged cells. Then, the battery cells are balanced in 1170 seconds, which is 19 minutes and 30 seconds. After the balance operation is finished, the final voltage values are 3.715. The second attempt is plotted in Figure 21 (b). Before the balance operation is started, the cell voltages are 3.797 V, 3.476 V, 3.355 V, 3.310 V, 3.604 V, 3.583 V, 3.510 V and 3.688 V, respectively. The estimated SoC difference between the highest and lowest charged cell voltages is calculated as 51.32%. After the balance operation is finished, the cell voltages are 3.559±0.01 V. The balance operation time is around 3033 seconds, which is 50 minutes and 33 seconds.

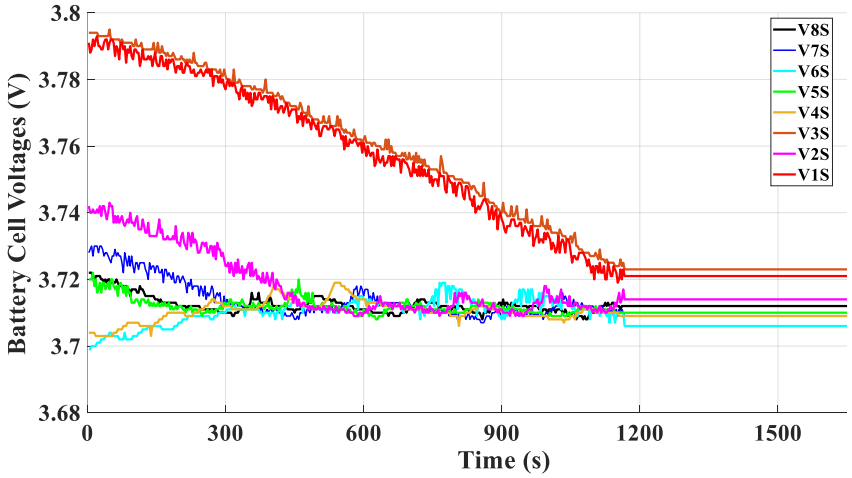

(a)

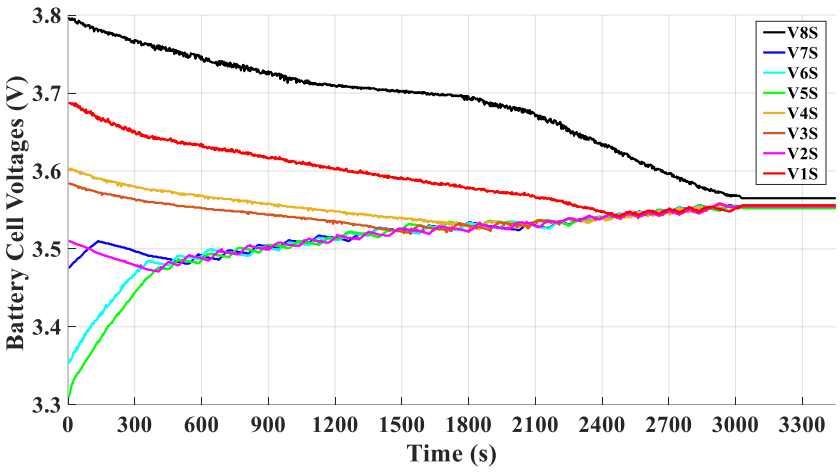

(b)

Figure 21. (a) First experimental result of battery balancing, (b) Second experimental result of battery balancing ((a) Batarya dengelemenin ilk deneysel sonucu, (b) Batarya dengelemenin ikinci deneysel sonucu)

4.6. Comparison with Other BMS Topologies
(Diğer BMS topolojileri ile karşılaştırma)

The comparison of the P2C studies by means of balancing speed, balancing efficiency and complexity is given in Table 3. The balancing speed values are estimated by dividing the reported voltage by the balance times. In addition, the reported SoC differences and a SoC graph in several papers are converted into voltage differences to compare their performances, as well. The proposed topology has the highest balancing speed thanks to the high power ability of the PI controlled ICC and up to four cells selection ability of the SWM with moderate efficiency. The complexity of the proposed topology is simpler since a single transformer is used, and the cell selection switches are not driven with PWM.

Table 3. Comparisons of balancing speed, efficiency and control difficulty for the proposed study with topologies in literature (Önerilen çalışma için dengeleme hızı, verimlilik ve kontrol zorluğunun literatürdeki topolojilerle karşılaştırılması)

P2C Studies in Literature	Balancing Speed	Efficiency	Complexity
Multiple transformer [25]	7.60mV/min Very high	90% High	Complex
Half bridge converter [26]	3.73mV/min Medium	90% High	Complex
Half Bridge converter [27]	8.33mV/min Very high	87% Medium	Moderate
Cell selective flyback [28]	2.51mV/min Low	99.91% Very high	Simple
Proposed cell selective ICC	9.63mV/min Very high	81.98% Medium	Simple

The cost effectiveness and size of the topologies that are presented in Table 4 are calculated by applying the analysis method presented in [41]. The cost of each component is defined as the constant values that are given, and the total cost is calculated by counting the components that are used for each of the 8 cells. Also, the size of the topologies is compared by considering the number of components used and their reported dimensions. Because the ICC topology has only one transformer,

the cost significantly drops, and the size of the topology is decreased. In addition, the passive components of ICC and the semiconductors of SWM tolerate the increase in cost and size as compared to the other topologies. As a result, the comparison of the proposed topology is more cost effective and ensures a smaller size.

Table 4. Comparison of cost and size for the proposed study with topologies in literature (Önerilen çalışma için maliyet ve boyutun literatürdeki topolojilerle karşılaştırılması)

Topology	Component Counts for Each 8 Cells								Cost ($)	Size
	M	RL	D	RS	L	C	T	MT		
Multiple transformer [25]	16	0	0	0	0	0	8	0	56.00	Large
Half bridge converter [26]	18	0	0	0	0	18	0	1	42.40	Large
Half bridge converter [27]	4	0	16	0	16	20	2	0	49.20	Large
Cell selective flyback [28]	19	0	20	1	0	1	2	0	33.90	Medium
Proposed cell selective ICC	18	0	16	0	2	4	1	0	31.40	Medium

Component price per unit ($): MOSFET and MOSFET driver IC (M) (0.2+0.8), relay (RL) (0.2), resistor (RS) (0.1), diode (D) (0.2), inductor (L) (1), capacitor (C) (0.8), single transformer (T) (5), multi-winding transformer (MT) (10)

5.CONCLUSIONS (SONUÇLAR)

This study investigates the implementation and performance of a proposed P2C BMS active balance topology with switch matrix. The design is simulated using MATLAB Simulink and subsequently validated through experimental implementation. The ICC and switch matrix are employed to facilitate charge transfer from the battery pack to individual cells, performing as anticipated. The study highlights that P2C active balance methods are capable of handling higher balance currents, which in turn accelerates the balancing operation. The SoC curve of the battery cells is estimated using a combination of the OCV method, measured DoD curves, and internal resistance estimation methods. Two different SoC configurations are tested in an idle state to demonstrate battery balance operation. The first configuration involves a 10% SoC difference, while the second involves a 55% SoC difference. These differences are balanced in 1170 seconds and 3033 seconds, respectively. The proposed system successfully balances low charged cells with the highest balancing speed among the compared topologies. The efficiency of the balance operation is evaluated and revealed as 81.98% at a current level of 3A during experimental tests. The SWM plays a critical role in selecting low charged cells from 1S to 4S, as detected in series, ensuring effective charge redistribution. The experimental results corroborate the simulation outcomes, demonstrating the robustness and speed of the proposed active balancing topology. These findings suggest that the proposed P2C BMS topology is a viable solution for enhancing the performance and longevity of battery systems by ensuring faster charge balancing. In addition to the speed, the proposed study provides cost effectiveness and a relatively smaller size among the P2C topologies. This research contributes to the advancement of BMS technology, providing a foundation for future developments aimed at optimizing battery performance and extending the operational lifespan of battery packs.

DECLARATION OF ETHICAL STANDARDS (ETİK STANDARTLARIN BEYANI)

The authors of this article declares that the materials and methods they use in their work do not require ethical committee approval and/or legal-specific permission.

Bu makalenin yazarı çalışmalarında kullandıkları materyal ve yöntemlerin etik kurul izni ve/veya yasal-özel bir izin gerektirmediğini beyan ederler.

AUTHORS' CONTRIBUTIONS (YAZARLARIN KATKILARI)

***Alperen UĞURLUOĞLU*:** He conducted the simulation and experimental studies, analyzed the results and performed the writing process.

Simülasyon ve deneysel çalışmaları yapmış, sonuçlarını analiz etmiş ve makalenin yazım işlemini gerçekleştirmiştir.

***Ahmet KARAARSLAN*:** He controlled the process of simulation and experimental studies and took part in monitoring the publication process.

Simülasyon ve deneysel çalışmaların süreçlerini kontrol etti ve yayın sürecinin takibinde yer aldı.

CONFLICT OF INTEREST (ÇIKAR ÇATIŞMASI)

There is no conflict of interest in this study.

Bu çalışmada herhangi bir çıkar çatışması yoktur.

REFERENCES (KAYNAKLAR)

[1] Clarke M, Alonso JJ. Lithium–ion battery modeling for aerospace applications. Journal of Aircraft. 2018; 58.6: 1323-1335.

[2] Al-Ismail FS, Alam M S, Shafiullah M, Hossain MI, Rahman SM. Impacts of renewable energy generation on greenhouse gas emissions in Saudi Arabia: A comprehensive review. Sustainability. 2023; 15(6): 5069.

[3] Liang Y, Zhao CZ, Yuan H, Chen Y, Zhang W, Huang JQ, Zhang, Q. A review of rechargeable batteries for portable electronic devices. InfoMat. 2019; 1(1): 6-32.

[4] AVCI G, ÖZDEMİR A. Recycling of Spent LFP Batteries. Gazi Üniversitesi Fen Bilimleri Dergisi Part C: Tasarım ve Teknoloji. 2023; 11(4).

[5] Fichtner M, Edström K, Ayerbe E, Berecibar M, Bhowmik A, Castelli IE, Weil M. Rechargeable batteries of the future—the state of the art from a BATTERY 2030+ perspective, Advanced Energy Materials 2022; 12(17): 2102904.

[6] Cetinkaya U, Bayındır R, Avcı E, Ayık S. Battery Energy Storage System Sizing, Lifetime and Techno-Economic Evaluation for Primary Frequency Control: A Data-driven Case Study for Turkey. Gazi University Journal of Science Part C: Design and Technology. 2022; 10(2): 177-194.

[7] Zeng X, Li M, Abd El-Hady D, Alshitari W, Al-Bogami AS, Lu J, Amine K. Commercialization of lithium battery technologies for electric vehicles, Advanced Energy Materials. 2019; 9(27): 1900161.

[8] Andrea D. Lithium-Ion Batteries and Applications: A Practical and Comprehensive Guide to Lithium-Ion Batteries and Arrays, from Toys to Towns Volume 2. Applications (Vol. 2), Artech House. 2020.

[9] Koyuncu MA, Taşdelen K. AKÜ YÖNETİM SİSTEMİNİN GELİŞTİRİLMESİ VE CANBUS VERİ TRAFİĞİNİN İNCELENMESİ. Gazi University Journal of Science Part C: Design and Technology. 2022; 10(4): 884-894.

[10] Lelie M, Braun T, Knips M, Nordmann H, Ringbeck F, Zappen H, Sauer DU. Battery management system hardware concepts: An overview. Applied Sciences. 2018; 8(4): 534.

[11] Gabbar HA, Othman AM, Abdussami MR. Review of battery management systems (BMS) development and industrial standards. Technologies. 2021; 9(2): 28.

[12] Kaliaperumal M, Dharanendrakumar MS, Prasanna S, Abhishek KV, Chidambaram RK, Adams S, Reddy MV. Cause and mitigation of lithium-ion battery failure—A review. Materials. 2021; 14(19): 5676.

[13] Das UK, Shrivastava P, Tey KS, Idris MYIB, Mekhilef S, Jamei E, Stojcevski A. Advancement of lithium-ion battery cells voltage equalization techniques: A review. Renewable and Sustainable Energy Reviews. 2020; 134: 110227.

[14] Omariba ZB, Zhang L, Sun D. Review of battery cell balancing methodologies for optimizing battery pack performance in electric vehicles. IEEE Access. 2019; 7: 129335-129352.

[15] Turksoy A, Teke A, Alkaya A. A comprehensive overview of the dc-dc converter-based battery charge balancing methods in electric vehicles. Renewable and Sustainable Energy Reviews. 2020; 133: 110274.

[16] Uzair M, Abbas G, Hosain S. Characteristics of battery management systems of electric vehicles with consideration of the active and passive cell balancing process. World Electric Vehicle Journal. 2021; 12(3): 120.

[17] Kumar S, Rao SK, Singh AR, Naidoo R. Switched-Resistor Passive Balancing of Li-Ion Battery Pack and Estimation of Power Limits for Battery Management System. International Journal of Energy Research. 2023; 2023(1): 5547603.

[18] Sun W, Li Y, Liu L, Mai R. A switched-capacitor battery equalization method for improving balancing speed. IET Electric Power Applications. 2021; 15(5): 555-569.

[19] Dong G, Yang F, Tsui KL, Zou C. Active balancing of lithium-ion batteries using graph theory and A-star search algorithm. IEEE Transactions on Industrial Informatics. 2020; 17(4): 2587-2599.

[20] Dam SK, John V. Low-frequency selection switch based cell-to-cell battery voltage equalizer with reduced switch count. IEEE Transactions on Industry Applications. 2021; 57(4): 3842-3851.

[21] Shang Y, Zhang C, Cui N, Guerrero JM. A cell-to-cell battery equalizer with zero-current switching and zero-voltage gap based on quasi-resonant LC converter and boost converter.

IEEE Transactions on Power Electronics. 2014; 30(7): 3731-3747.

[22] Habib AA, Hasan MK. Lithium-ion battery state-of-charge balancing circuit using single resonant converter for electric vehicle applications. Journal of Energy Storage. 2023; 61: 106727.

[23] Shang Y, Cui N, Duan B, Zhang C. A global modular equalizer based on forward conversion for series-connected battery strings. IEEE Journal of Emerging and Selected Topics in Power Electronics. 2017; 6(3): 1456-1469.

[24] Imtiaz AM, Khan FH. "Time shared flyback converter" based regenerative cell balancing technique for series connected Li-ion battery strings. IEEE Transactions on power Electronics. 2013; 28(12): 5960-5975.

[25] McCurlie L, Preindl M, Emadi A. Fast model predictive control for redistributive lithium-ion battery balancing. IEEE Transactions on Industrial Electronics. 2016; 64(2): 1350-1357.

[26] Zilio A, Mattavelli P. A flexible Multi-Active Half-Bridge converter for active balancing of series-connected Li-Ion cells. In IECON 2021–47th Annual Conference of the IEEE Industrial Electronics Society, IEEE. 2021; 1-6.

[27] Uno M, Kukita A. String-to-battery voltage equalizer based on a half-bridge converter with multistacked current doublers for series-connected batteries. IEEE Transactions on Power Electronics. 2018; 34(2): 1286-1298.

[28] Guo X, Geng J, Liu Z, Xu X, Cao W. A flyback converter-based hybrid balancing method for series-connected battery pack in electric vehicles. IEEE Transactions on Vehicular Technology. 2021; 70(7): 6626-6635.

[29] Alam MA, Minai AF, Bakhsh FI. Isolated bidirectional DC-DC Converter: A topological review. e-Prime-Advances in Electrical Engineering. Electronics and Energy. 2024; 8: 100594.

[30] Hoque MM, Hannan MA, Mohamed A. Optimal algorithms for the charge equalisation controller of series connected lithium-ion battery cells in electric vehicle applications. IET Electrical Systems in Transportation. 2017; 7(4): 267-277.

[31] Ouyang Q, Chen J, Zheng J, Hong Y. SOC estimation-based quasi-sliding mode control for cell balancing in lithium-ion battery packs. IEEE transactions on industrial electronics. 2017; 65(4): 3427-3436.

[32] McCurlie L, Preindl M, Emadi A. Fast model predictive control for redistributive lithium-ion battery balancing. IEEE Transactions on Industrial Electronics. 2016; 64(2): 1350-1357.

[33] Khan N, Ooi CA, Alturki A, Amir M, Alharbi T. A critical review of battery cell balancing techniques, optimal design, converter topologies, and performance evaluation for optimizing storage system in electric vehicles. Energy Reports,. 2024; 11: 4999-5032.

[34] Feng F, Hu X, Liu J, Lin X, Liu B. A review of equalization strategies for series battery packs: variables, objectives, and algorithms. Renewable and Sustainable Energy Reviews. 2019; 116: 109464.

[35] Aboulnaga AA, Emadi A. High performance bidirectional Cuk converter for telecommunication systems. In INTELEC 2004. 26th Annual International Telecommunications Energy Conference, IEEE. 2004, September; 182-189.

[36] Olabi AG, Abbas Q, Shinde PA, Abdelkareem MA. Rechargeable batteries: Technological advancement, challenges, current and emerging applications. Energy. 2023; 266: 126408.

[37] Ko G, Jeong S, Park S, Lee J, Kim S, Shin Y, Kwon K. Doping strategies for enhancing the performance of lithium nickel manganese cobalt oxide cathode materials in lithium-ion batteries. Energy Storage Materials. 2023; 102840.

[38] Habib AA, Hasan MK, Issa GF, Singh D, Islam S, Ghazal TM. Lithium-ion battery management system for electric vehicles: constraints, challenges, and recommendations. Batteries. 2023; 9(3): 152.

[39] Hannan MA, Lipu MH, Hussain A, Mohamed A. A review of lithium-ion battery state of charge estimation and management system in electric vehicle applications: Challenges and recommendations. Renewable and Sustainable Energy Reviews. 2017; 78: 834-854.

[40] Riczu C, Bauman J. Implementation and system-level modeling of a hardware efficient cell balancing circuit for electric vehicle range extension. IEEE Transactions on Industry Applications. 2021; 57(3): 2883-2895.

[41] Shang Y, Zhang Q, Cui N, Duan B, Zhou Z, Zhang C. Multicell-to-multicell equalizers based on matrix and half-bridge LC converters for series-connected battery strings. IEEE Journal of Emerging and Selected Topics in Power Electronics. 2019; 8(2): 1755-1766.